Intramolecular dynamics by photoelectron spectroscopy. I. Application to N+ 2, HBr+, and HCN+

A. J. Lorquet, J. C. Lorquet, J. Delwiche, and M. J. Hubin-Franskin

Citation: The Journal of Chemical Physics **76**, 4692 (1982); doi: 10.1063/1.442785
View online: http://dx.doi.org/10.1063/1.442785
View Table of Contents: http://scitation.aip.org/content/aip/journal/jcp/76/10?ver=pdfcov
Published by the AIP Publishing

Intramolecular dynamics by photoelectron spectroscopy. I. Application to N_2^+, HBr^+, and HCN^+

A. J. Lorquet, J. C. Lorquet, J. Delwiche,[a] and M. J. Hubin-Franskin[a]

Département de Chimie, Universite de Liege, Sart-Tilman, B-4000 Liege 1, Belgium
(Received 25 November 1982; accepted 19 January 1982)

The Fourier transform of an optical electronic spectrum leads to an autocorrelation function $C(t)$ which describes the evolution in time of the wave packet created by the Franck–Condon transition, as it propagates on the potential energy surface of the electronic upper state. This correlation function is equal to the modulus of the overlap integral between the initial position of the wave packet and its instantaneous position at time. The original data resulting from an experimentally determined spectral profile must be corrected for finite energy resolution, rotational, and spin-orbit effects. The behavior of the system can then be followed up to a time of the order of 10^{-13} s, i.e., during the first few vibrations which follow immediately the electronic transition. The method is applied to photoelectron spectra and the results are compared to the available information on potential energy surfaces of ionized molecules, in order to study their unimolecular dissociation dynamics. In the case of the $X\,^2\Sigma_g^+$, $A\,^2\Pi_u$, and $B\,^2\Sigma_u^+$ states of N_2^+, an oscillatory pattern is obtained for the correlation function. This indicates that the nuclear motion is taking place in a bound potential. Effects due to anharmonicity are visible in the case of the $A\,^2\Pi_u$ state. The study of the $X\,^2\Pi$ state of HBr^+ demonstrates the overwhelming importance of spin-orbit coupling when heavy atoms are present in the molecule. Finally, the method is applied to a polyatomic molecule. The potential energy surface of the $\tilde{B}\,^2\Sigma^+$ state of HCN^+ is characterized by two energy minima separated by a saddle point. The corresponding band in the photoelectron spectrum is characterized by an irregular vibrational structure superimposed upon a broad continuum. A study of the correlation function shows that the wave packet undergoes a complicated, two-component motion: while oscillating across the saddle point, it spreads away at the same time along the dissociative degree of freedom. This gives information on the rate of energy redistribution within the molecule.

I. INTRODUCTION

Dynamic processes are often studied in terms of a rate expression involving one or several rate constants. There exists, however, an alternative formulation in which they are described in terms of a time autocorrelation function.[1,2] These functions indicate how long some given property of a system persists until it is averaged out by a dynamic process. They can, in principle, be calculated from a model, but it is possible and much more convenient to obtain them directly from experiment, as the Fourier transform of the spectral profile of an absorption or emission band. The method is well known in various fields of molecular spectroscopy,[2,3] especially, NMR, IR, and Raman, and has provided a wealth of information on intermolecular forces. It is, however, quite general and not limited to the study of systems undergoing random or stochastic processes.

Quite recently, the significance of a correlation function $C(t)$ in an electronic spectroscopy experiment (i.e., the significance of the Fourier transform of an electronic band) has been elucidated by Heller.[4] He showed that the Fourier transform of an electronic absorption band profile $I(E)$ was equal to an overlap integral between two nuclear wave functions ϕ and $\phi(t)$:

$$\langle \phi \,|\, \phi(t) \rangle = \int_{-\infty}^{+\infty} \frac{I(E)}{E}\, e^{-iEt/\hbar}\, dE \Big/ \int_{-\infty}^{+\infty} \frac{I(E)}{E}\, dE \,, \quad \text{(I.1)}$$

where ϕ is the nuclear wave function of the ground state prepared on the potential energy surface of an upper electronic state by a vertical Franck–Condon transition, and $\phi(t)$ is the wave packet at time t as it moves away from its initial position ϕ on the potential energy surface of the upper state. The denominator in Eq. (I.1) ensures that the correlation function is normalized to unity at time $t=0$. We shall henceforth consider a correlation function $C(t)$ which is equal to the modulus of this overlap integral

$$C(t) = \left| \langle \phi \,|\, \phi(t) \rangle \right| \,. \quad \text{(I.2)}$$

Equation (I.1) is more simply derived in the Appendix.

Heller proposed to calculate $\langle \phi \,|\, \phi(t) \rangle$ from a swarm of classical trajectories on a given potential energy surface in order to account for observed spectral profiles. What we would like to do in the present series of papers is the opposite: i.e., start from experimentally observed spectra of specific molecules and extract from them a dynamic information which then should be related to the shape of the potential energy surface of the relevant electronic state (or states). In principle, the Fourier transform of an experimental spectroscopic profile leads directly to the desired information. In practice, however, it is necessary to correct the data for a number of additional factors (finite energy resolution, overall molecular rotation, spin-orbit splitting) in the treatment of the experimental data. These corrections are examined in the next section.

The method can be applied to any dipolar electronic transition. It provides information on the 10^{-15}–10^{-13} s range, and illustrates Bohr's complementarity principle,[5,6] according to which a full description of a physi-

[a] Chercheur Qualifié du Fonds National de la Recherche Scientifique, Belgium.

 0021-9606/82/104692-08$02.10

cal system can only be obtained if the results of two different sets of observations (corresponding to high energy resolution and sharp time definition, respectively) are put together.

In the present series of papers, we have chosen to apply the method to the case of photoelectron spectroscopy in order to study the unimolecular dissociation dynamics of ionized molecules in the femtosecond range.[7] Other techniques have been developed to study the further evolution of a molecular ion at longer times (from 10^{-12} to 10^{-6} and even 10^{-3} s).[8] If all the available techniques were applied to a given ionic system (preferably one whose potential energy surfaces are known[9] or whose reaction paths have been determined[10]), a complete account of the dissociation process from the first initial molecular vibration up to a time of 10^{-6} and even 10^{-3} s would be obtained. A real breakthrough in our understanding of unimolecular dissociation dynamics would result.

II. DATA HANDLING

A. Energy resolution

The quality of a correlation function $C(t)$ deteriorates with time. The information becomes unreliable at times larger than $\hbar/\Delta E$, where ΔE is the energy resolution. With $\Delta E = 10$ meV, the time limit is equal to 6.6×10^{-14} s, roughly equal to six CH stretching or to two CC stretching vibrational periods. Such an energy resolution is currently difficult to obtain. However, the situation can be considerably improved by appropriate data handling.

In photoelectron spectroscopy, the energy resolution is determined from the experimental profile of a rare gas added to the substance under study. More precisely, the profile of any peak can be expressed as a convolution integral between the real profile and an apparatus function, which is simulated by the rare gas profile. Then, as a result of a well-known theorem on convolution integrals,[11] the real correlation function can be expressed as a ratio between the Fourier transform of the experimental band profile and the Fourier transform of the reference rare gas peak. The correction is, however, approximate, since peak broadening results from effects which are not exactly the same in the reference rare gas and in the molecule under study. Further details will be given in Sec. III.

B. Molecular rotation

The nuclear wave functions ϕ and $\phi(t)$, whose overlap integral determines the correlation function, can, to a good approximation, be factorized into a vibrational and a rotational part. Then,

$$\langle\phi\,|\,\phi(t)\rangle = \langle\phi^{\mathrm{rot}}\,|\,\phi^{\mathrm{rot}}(t)\rangle\langle\phi^{\mathrm{vib}}\,|\,\phi^{\mathrm{vib}}(t)\rangle\ ,$$
$$C(t) = C^{\mathrm{rot}}(t)\cdot C^{\mathrm{vib}}(t)\ . \qquad \text{(II. 1)}$$

Only the vibrational part of the correlation function provides information on the shape of the potential energy surface. This means that the Fourier transform of the experimental band profile must again be divided by the correlation function of a molecular rotor in order to obtain the vibrational part of the correlation function, i.e., $C^{\mathrm{vib}}(t)$.

The correlation function of a freely rotating molecule has a simple expression in the case of linear[2] and spherical[12] tops. More complicated expressions have been proposed by various authors[13–15] in the case of symmetric tops. However, at times shorter than $\tau^* = (I/kT)^{1/2}$, all these expressions are very close to a simple Gaussian law[12]

$$C^{\mathrm{rot}}(t) \simeq \exp[-(kT/I)t^2]\ , \qquad \text{(II. 2)}$$

where I is the moment of inertia.

The time limit τ^* is equal to 6.5×10^{-14} s in the case of a diatomic hydride such as HBr (the worst case) and to 1.8×10^{-13} s in the case of N_2.

In the case of correlation functions obtained from IR spectra, Eq. (II. 2) has been found to give good results up to a time of at least 10^{-13} s, irrespective of the shape of the molecule.[16–18]

C. Spin-orbit splitting

In the electronic transition, the initial state is usually a singlet, but, because of spin-orbit splitting, the final state may be a multiplet, e.g., a $^2\Pi$ state. Then, the measured photoelectron spectrum consists of two identical components $I_1(E)$ and $I_2(E)$, which are separated in energy by a quantity Ω.

$$I(E)/E = I_1(E)/E + I_2(E)/E$$
$$= I_1(E)/E + I_1(E+\Omega)/(E+\Omega)\ . \qquad \text{(II. 3)}$$

Substituting into Eq. (I. 1), the correlation function is then given by

$$\langle\phi\,|\,\phi(t)\rangle = \left\{\int_{-\infty}^{+\infty} e^{-iEt/\hbar}\frac{I_1(E)}{E}\,dE + \int_{-\infty}^{+\infty}\exp[-i(E-\Omega)t/\hbar]\frac{I_1(E)}{E}\,dE\right\}\Big/\int_{-\infty}^{+\infty}\frac{I_1(E)}{E}$$
$$= (1+e^{i\Omega t/\hbar})\int_{-\infty}^{+\infty} e^{-iEt/\hbar}\frac{I_1(E)}{E}\,dE\Big/\int_{-\infty}^{+\infty}\frac{I_1(E)}{E}\,dE\ . \qquad \text{(II. 4)}$$

Comparing with Eq. (I. 1), one sees that the presence of a spin-orbit splitting Ω introduces an additional factor, which, in modulus, is equal to

$$(1+e^{i\Omega t/\hbar}) = 2\,|\cos(\Omega t/2\hbar)|\ . \qquad \text{(II. 5)}$$

Thus, the experimental correlation function contains an oscillatory factor. The larger the spin-orbit splitting, the faster the oscillations. If the molecule contains a heavy atom such as Br or I, the influence of this factor becomes predominant, as will be seen in Sec. IV C.

D. Anharmonicity

A Gaussian wave packet moving in an anharmonic potential undergoes various distortions. Most of the time, it broadens and flattens (although in some cases it may also get sharper). It may even break up[19] if the

anharmonicity is large enough. As a result, when the wave packet moves back towards its initial position, the overlap is reduced with respect to its initial value. In other words, the recurrences (if any) are characterized by maxima of the correlation function, but the value of the maxima are less than unity.

No convenient analytical treatment exists to describe the influence of anharmonicity on the motion of a wave packet, even in the case of a diatomic molecule. However, some idea of the wave packet flattening can be obtained empirically as follows. At time $t=0$, the wave packet ϕ has an average velocity equal to zero and hence can be represented by the expression

$$\phi = h_1 \exp[-(1/2)(q/\sigma_1)^2] \qquad \text{(II. 6)}$$

if its height is h_1 and its half-width $\Gamma_1 = 2.354\,\sigma_1$. Let us assume that it flattens as time goes on while retaining a Gaussian shape throughout its evolution. Its surface is constant and remains equal to $\sqrt{2\pi}\,h_1\sigma_1$. At the beginning of the nth oscillatory cycle, the traveling wave packet is again at rest and can be represented by an expression analogous to Eq. (II. 6) with parameters now equal to h_n and σ_n. The correlation function then reaches a maximum which is readily calculated as an overlap integral. Its value is equal to

$$C_n = (h_1\sigma_1)^2/(\sigma_1^2+\sigma_n^2)^{1/2} \quad . \qquad \text{(II. 7)}$$

Let $\rho_n = C_n/C_1$ represent the value of the correlation function at the nth recurrence normalized with respect to its value at time $t=0$.

Then,

$$(h_n/h_1) = [\rho_n^2/(2-\rho_n^2)]^{1/2} \quad . \qquad \text{(II. 8)}$$

E. Conclusions

In summary, information on the motion of the wave packet on the potential energy surface of the upper state can be obtained by a study of the modulus of the vibrational part of the autocorrelation function. Summing up the various corrections, one has, finally,

$$C^{\text{vib}}(t) = |\langle\phi^{\text{vib}}|\,\phi^{\text{vib}}(t)\rangle| = \left\{\left|\int_{-\infty}^{+\infty}[I(E)/E]\,e^{-iEt/\hbar}\,dE\right| \Big/ \int_{-\infty}^{+\infty}[I(E)/E]\,dE \Big/ \left|\int_{-\infty}^{+\infty}[I^{\text{rg}}(E)/E]\,e^{-iEt/\hbar}\,dE\right|\right\}$$
$$\times \exp[(kT/I)t^2] \times (|\cos(\Omega t/2\hbar)|)^{-1} \quad , \qquad \text{(II. 9)}$$

where $I(E)$ and $I^{\text{rg}}(E)$ refer to the intensities of the studied electronic band and of the reference rare gas, respectively.

III. EXPERIMENTAL

The photoelectron spectra analyzed in this paper were recorded with a hemispherical electrostatic analyzer characterized by a mean radius of 5.5 cm, a total slit width of 2.5 mm, a kinetic energy of analysis of 0.8 eV, and a calculated resolution (FWHM) of 0.0182 eV. As the spectrometer is operated in the constant energy mode, this resolution should remain constant over the whole energy range.[20] Several factors exist, however, that contribute to worsen the resolution: (i) linewidth of the photon beam; (ii) Doppler effect; (iii) rotational broadening; (iv) various effects such as spurious potentials resulting from adsorbed substances on the surfaces (surface potentials), inhomogeneity of the residual magnetic field, mechanical misalignment, and distortion in the electrical fields; and (v) shifts of surface potentials with time and pressure.

The magnitude of these different factors have been discussed in detail by many authors, and especially by Dehmer and Dehmer,[21] and by Rabalais.[22] We shall therefore restrict ourselves to the points that are relevant for our purpose.

It is of common practice to take into account points (i) and (iv) by recording the photoelectron spectrum of a rare gas simultaneously with that of the compound under study. This is realized by mixing the rare gas to the compound in the collision chamber. The shape of the rare gas peak is generally considered to represent the experimental apparatus function. Regarding point (ii), there exists a theoretical formula giving the magnitude of the Doppler effect. A study of mixtures of rare gases revealed, however, that the linewidths of rare gas peaks do not strictly follow the expected law. The reason for this is not fully understood. In practice, good results were obtained by using a rare gas whose peak is located as close as possible to the electronic band under investigation. Shifts of contact potentials [point (v)] are far more difficult to take into account. To minimize their effects, it is essential to record the spectra in as short a time as possible. Finally, it is not advisable to increase the pressure too much in order to improve the signal-to-noise ratio. Figure 1 shows

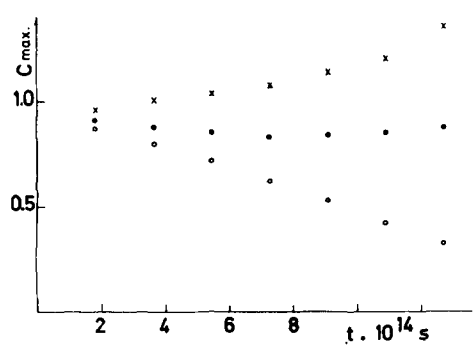

FIG. 1. Maxima of the correlation function of the $A\,^2\Pi_u$ state of N_2^+ after correction for finite resolution, rotation, and spin-orbit coupling effects. Black dots: spectra taken under optimal conditions. Open circles: spurious decrease due to excessive accumulation time. Crosses: spurious increase due to excessive pressure in the vacuum chamber.

results for N_2 obtained from spectra recorded at various pressures and with different accumulation times. As expected from the previous discussion, long accumulation times and excessive pressures lead to poor results. In practice, we found that the accumulation time should not exceed 1.5 h while keeping the pressure in the 10^{-6} Torr range in the vacuum chamber.

As the electrons are decelerated before entering the analyzer, the spectra have to be corrected for the transmission efficiency of the decelerating system. This is accomplished by multiplying the intensity at each point by the corresponding electron energy.[23]

Since the spectra had to be recorded in a short time, the signal-to-noise ratio was not favorable. It was improved by smoothing the data using a parabolic least square fitting on five points.[24] The best results were obtained with five smoothing cycles. This procedure does not alter[25] the intensity ratios of the peaks in the band, provided that the peaks are defined by a sufficiently large number of points (at least ten times the number of points on which the fitting is calculated).

No correction for the influence of the asymmetry factor β of the angular distribution of the photoelectrons has been introduced. As our analyzer is fitted with 5 mm long inlet and exit slits, the total angle of acceptance for the photoelectrons is approximately 60°. Therefore, it is expected that the variation of β within the energy range of an electronic band will be negligible.

IV. RESULTS

A. The $X\,^2\Sigma_g^+$ and $B\,^2\Sigma_u^+$ states of N_2^+

Let us consider first the simplest possible case: a diatomic molecule which is ionized to a bound state characterized by a high dissociation energy and an equilibrium distance nearly equal to that of the neutral ground state. The vibrational amplitude is then small and anharmonicity can be neglected. The photoelectron spectrum consists of an intense 0–0 transition followed by much weaker vibrational peaks. Examples of this situation can be found in the $X\,^2\Sigma_g^+$ and $B\,^2\Sigma_u^+$ states of N_2^+ (Fig. 2).

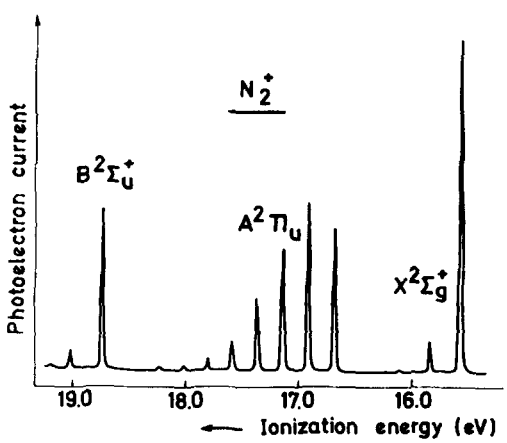

FIG. 2. HeI (58.4 nm) photoelectron spectrum of the $X\,^2\Sigma_g^+$, $A\,^2\Pi_u$, and $B\,^2\Sigma_u^+$ ionic states of nitrogen.

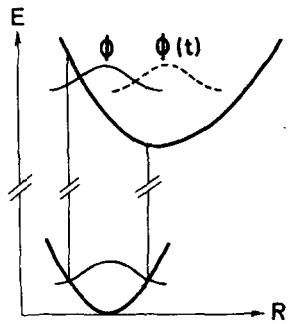

FIG. 3. A Franck–Condon transition leads to a wave packet ϕ, which propagates on the potential energy surface of the upper electronic state.

The vibrational correlation function $C^{vib}(t)$ is then a periodic function of time. The overlap integral oscillates between a maximum value of one (when the traveling wave packet overlaps its initial position) and a minimum value which measures the overlap at maximum stretching, i.e., after an odd number of vibrational half-periods (Fig. 3).

In the case of the X and B states of N_2^+, the internuclear equilibrium distances ($R_X^{eq} = 1.116$ Å; $R_B^{eq} = 1.075$ Å) are close to that of the ground state of the neutral molecule ($R^{eq} = 1.098$ Å). As a result, the vibrational amplitudes are small and the minimal overlaps are large. The experimental time correlation functions corresponding to these two cases are represented in Figs. 4 and 5. The dotted line represents the direct Fourier transform of the photoelectron spectrum with no correction applied. The dashed line represents the data corrected for finite resolution (i.e., after division by the Fourier transform of the $^2P_{3/2}$ peak of Kr^+). There is no spin-orbit coupling correction in this case since one is dealing with $^2\Sigma$ states. The solid line represents the final correlation function after correction for molecular rotation, i.e., after division by Eq. (II.2).

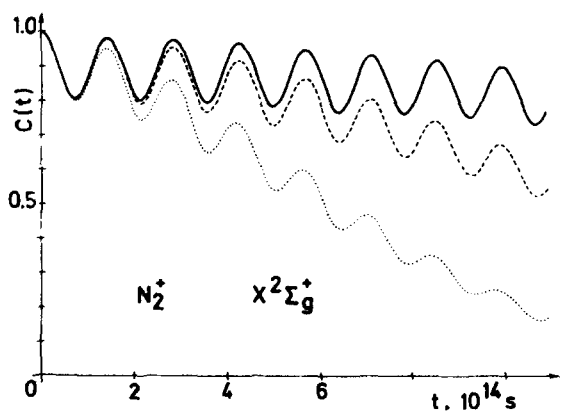

FIG. 4. Correlation function of the $X\,^2\Sigma_g^+$ state of N_2^+. Dotted line: Fourier transform of the experimental photoelectron spectrum. Dashed line: correlation function corrected for finite energy resolution. Solid line: same after correction for rotation.

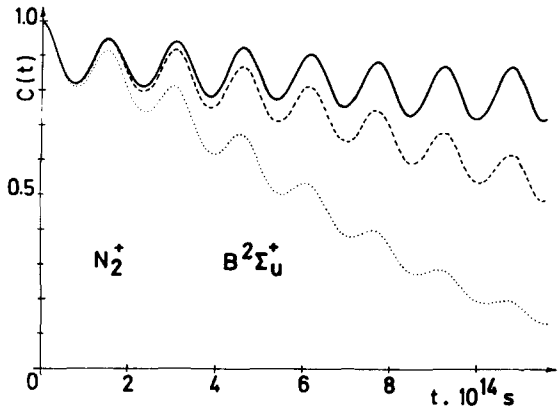

FIG. 5. Correlation function of the $B^2\Sigma_u^+$ state of N_2^+. Dotted line: Fourier transform of the experimental photoelectron spectrum. Dashed line: correlation function corrected for finite energy resolution. Solid line: same after correction for rotation.

A value of one for the maximum overlap is not strictly recovered after each vibrational cycle. The values range between 1 and 0.87. Two explanations can be given. Firstly, the effect could be due to the approximate nature of the corrections for finite resolution and for overall rotation. Secondly, it is well known that a Gaussian wave packet vibrating in a harmonic potential remains unchanged[26] provided its shape is identical with the vibrationless wave function of the potential in which it oscillates. But this is not necessarily the case for a Gaussian wave packet oscillating in a slightly anharmonic potential with a different curvature, as in the case of a Franck–Condon transition. Classical trajectory calculations are under way to study this in more detail.

B. The $A\,^2\Pi_u$ state of N_2^+

In the case of this state, the Fourier transform has to be additionally corrected for spin-orbit splitting ($\Omega = 74.6\ \text{cm}^{-1} = 0.009$ eV). This effect is too small to be seen in the direct photoelectron spectrum but, as shown in Fig. 6, it is not at all negligible when the Fourier transform is considered. The difference between the dot–dash and the solid lines, obtained before and after correction, gives the importance of this effect.

Furthermore, the state is characterized by an equilibrium internuclear distance of 1.174 Å, whereas that of the ground state of the neutral molecule is 1.098 Å. The corresponding photoelectron band is characterized by a substantial vibrational excitation: the Franck–Condon zone extends up to the 0–8 transition. Correspondingly, the minimal values of the correlation functions which measure the overlap at maximum stretching is ten times smaller for the A state than for states X and B. Since the amplitude of the vibrational motion is large, anharmonicity effects are expected to be important.

Using Eq. (II.8), the relative height of the wave packet can be evaluated at the beginning of each oscillation. For the A state of N_2^+, h_2/h_1 is equal to 0.84. The further oscillations still lead to a decrease, but the effect is less important. A similar observation can be made for the other states of N_2^+. h_2/h_1 is equal to 0.91 for the X state and 0.97 for the B state. These values illustrate the fact that, the smaller the amplitude of the vibrational motion, the smaller the anharmonicity, and the less important the flattening of the wave packet.

One notices the presence in the correlation function of small additional peaks whose intensity increases with time. This puzzling pattern is very reproducible and is affected neither by the algorithm used in the Fourier transformation nor by the assumptions made in the treatment of experimental data: noise removal, shift of base line, background correction, etc. These additional maxima are not due to an insufficient number of experimental points in the determination of the spectral profile (no "aliasing effect"[27]).

A study of model spectra revealed that they resulted from the unequal energy spacing in the vibrational progression. In other words, the additional maxima are due to anharmonicity. We thus interpret them as evidence for wave packet splitting in an anharmonic potential.[19]

C. The $X\,^2\Pi_i$ state of HBr^+

This state is characterized by a very important spin-orbit splitting. The corresponding band of the photoelectron spectrum (Fig. 7) results from the superposition of two components. As a consequence, the correlation function is largely determined by the oscillatory factor characteristic of spin-orbit splitting [Eq. (II.5)]. In other words, the final result depends in a very sensitive way on the value assumed for Ω. For inappropriate values of Ω, discontinuities appear which may be so sharp as to conceal the existence of maxima and minima of the correlation function. A value of $2651.3 \pm 2\ \text{cm}^{-1}$ for Ω was found to minimize the discontinuities. It is very close to the spectroscopic value of $2651.6\ \text{cm}^{-1}$.[28]

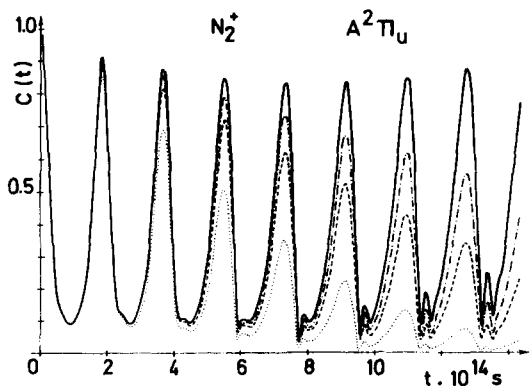

FIG. 6. Correlation function of the $A\,^2\Pi_u$ state of N_2^+. Dotted line: Fourier transform of the experimental photoelectron spectrum. Dashed line: correlation function after correction for finite energy resolution. Dot–dash line: same after correction for rotation. Solid line: final correlation function after correction for spin-orbit coupling.

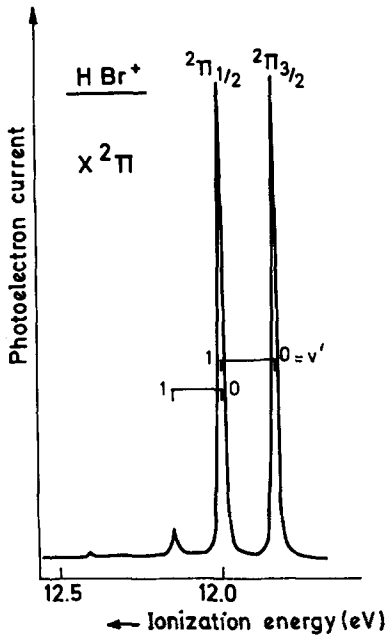

FIG. 7. HeI (58.4 nm) photoelectron spectrum of the ionic ground state $X\,^2\Pi_i$ of hydrogen bromide.

Removal of the oscillatory factor [the last term in Eq. (II.9)] leads to a pure vibrational correlation function (the solid line of Fig. 8), whose information content (and in particular the vibrational frequency) is much more easily deciphered than that of the direct energy spectrum.

D. The $\tilde{B}\,^2\Sigma^+$ state of HCN^+

Let us now turn to a polyatomic molecules. As an example, consider the case of the third electronic state $\tilde{B}\,^2\Sigma^+$ of HCN^+, whose potential energy surface has been calculated.[9] The corresponding band in the photoelectron spectrum (Fig. 9) shows an irregular pattern of

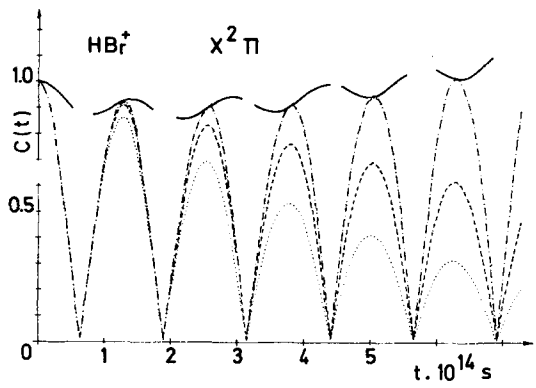

FIG. 8. Correlation function of the $X\,^2\Pi$ state of HBr^+. Dotted line: Fourier transform of the experimental photoelectron spectrum. Dashed line: correlation function after correction for finite energy resolution. Dot–dash line: same after correction for rotation. Solid line: final correlation function after correction for spin-orbit coupling. It has been interrupted to conceal the effects of the discontinuities occasioned by the oscillatory factor due to spin-orbit coupling (Eq. II.5).

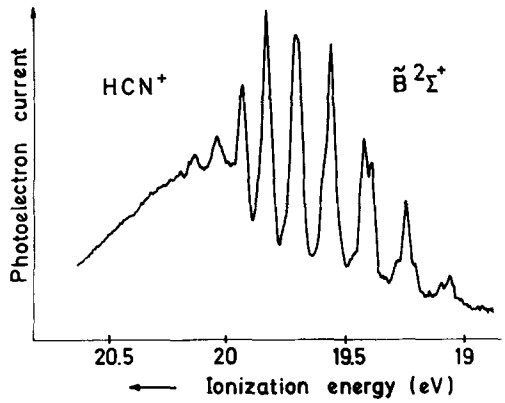

FIG. 9. HeI (58.4 nm) photoelectron spectrum of the $\tilde{B}\,^2\Sigma^+$ state of HCN^+ (third electronic band).

vibrational peaks superimposed upon a broad continuum. A direct interpretation of the frequency spectrum would be very hard.[9,29] Its Fourier transform, however, leads to a time correlation function which is much more easily interpreted and which provides, at the same time, interesting information concerning energy exchange among oscillators.

The potential energy surface[9] of the $\tilde{B}\,^2\Sigma^+$ state of HCN^+ is represented in Fig. 10. It is characterized by the presence of two energy basins separated by a saddle point. Basin A (towards large CH bond lengths) opens up into a dissociation valley ($H + CN^+$) and is further electronically predissociated.

This unusual shape of the potential energy surface

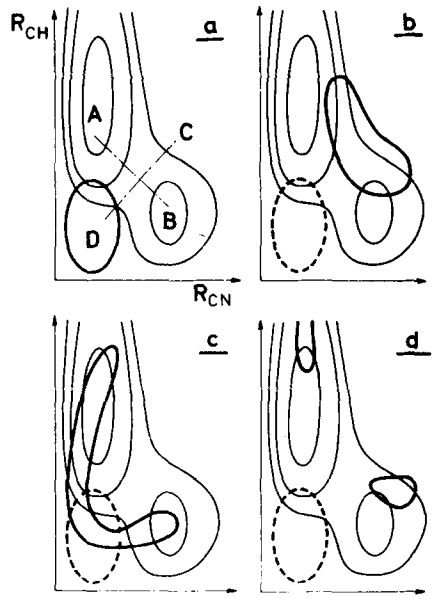

FIG. 10. Part (a): Potential energy surface of the $\tilde{B}\,^2\Sigma^+$ state of HCN^+. The Franck–Condon zone is shown as an ellipse which represents the initial position of the wave packet created by ionization. Parts (b), (c), and (d): schematic representation of the motion of the wave packet $\phi(t)$ on the potential energy surface. The wave packet oscillates along direction CD while spreading along coordinate AB.

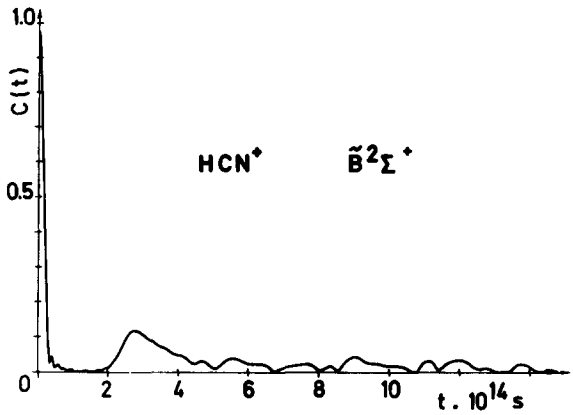

FIG. 11. Correlation function of the $\tilde{B}\ ^2\Sigma^+$ state of HCN^+.

provides a good example of the fact that the vibrational normal modes which are appropriate for an excited state are sometimes quite different from those of the ground state (Duschinsky effect[30]). Any discussion of the energy flow among normal modes should be made in terms of the former and not in terms of the latter.

In the case of HCN^+ in its $\tilde{B}\ ^2\Sigma^+$ state, the appropriate normal coordinates are: (i) in-phase stretching of both CH and CN bonds [direction CD in Fig. 10(a)], which is a bound degree of freedom; (ii) out-of-phase stretching of these two bonds [direction AB in Fig. 10(b)], which corresponds to a negative curvature and therefore connects the saddle point to either the dissociation valley or to the shallow basin B; (iii) the doubly degenerate bending mode (which in this particular example corresponds to a very flat potential and thus to a low frequency value).

The time correlation function is represented in Fig. 11. It is easily interpreted in terms of a diagram showing the evolution of the wave packet $\phi(t)$ as it propagates on the potential energy surface (Fig. 10). The initial position ϕ as determined by the Franck–Condon principle is represented by an ellipse in Fig. 10(a). The wave packet then executes a vibrational motion along direction CD while spreading away, at the same time, along coordinate AB. After one-half vibrational period (i.e., 1.4×10^{-14} s, as read in Fig. 11), the overlap (and thus the correlation function) is equal to zero [Fig. 10(b)]. The wave packet then comes backwards. However, the overlap is only equal to 0.12 after a complete vibrational period [Fig. 10(c) and Fig. 11 at $t=2.8\times10^{-14}$ s]. The reduction of the overlap results from the flattening of the wave packet. Flattening along the bound degree of freedom (CD axis) corresponds to a modification of the initial Franck–Condon distribution, i.e., to an intramolecular vibrational energy transfer among vibrational energy levels of the CD normal mode. The other source of flattening results from energy flow into the dissociative degree of freedom AB.

The overall reduction from one to 0.12 within 2.8×10^{-14} s corresponds to fast intramolecular energy transfer. The subsequent evolution is seen to take place much more slowly and according to a completely different pattern (Fig. 11). The reason is that the wave packet is then split into two parts [Fig. 10(d)]: one which travels along the dissociation channel, and another one which is trapped (at least temporarily) in the shallow minimum B and which executes vibrations of its own. These vibrations are responsible for the long time behavior of the correlation function (Fig. 11).

Thus, as far as intramolecular energy transfer is concerned, a study of the correlation function shows that the relaxation of the system is not governed by an exponential law with a single rate constant. Fast initial energy transfer is followed by a much slower subsequent evolution. The same conclusion emerges from a classical trajectory study of the $\tilde{B}\ ^2B_2$ state of H_2O^+.[31]

In summary, the correlation function leads to a simple dynamic picture, whereas no interpretation of the vibrational frequencies observed in the energy spectrum is possible in terms of the usual model. The reason is that the system executes complicated vibrations which have a simple explanation in terms of wave packet motion, but which have little to do with the normal modes of a set of harmonic oscillators. This illustrates the power of Heller's approach.

V. DISCUSSION

This work provides a striking example of the complementarity of spectroscopic and kinetic experimentation. What is essentially discussed here is the interplay between *two different experiments*, each of which provides a different information on the system. The more appropriate the experimental conditions for one of them, the poorer the information provided by the other. Hence, one deals with two experiments which are complementary in the sense defined by Bohr.[5,6]

In the spectroscopic experiment, the system is ideally prepared by nearly monochromatic photons. Every effort is made to achieve good energy resolution and little information concerning time evolution is available. In the kinetic experiment, the system is prepared by a very short pulse, whose construction requires superposition of a large number of energy states. Hence, the time resolution is very good, but the energy is poorly defined. (The energy spread extends over the whole Franck–Condon zone.)

It turns out that the former experiment is more easily done than the latter. But it is possible to go over to the other by Fourier transformation because both experiments depend on the same quantity (viz., the transition moment). Hence, it is possible to predict the result of a hypothetical kinetic experiment from an energy spectrum.

Spectroscopic experimentation can thus help us to study problems of intramolecular dynamics, such as wave packet propagation on potential energy surfaces, energy redistribution among normal modes, and fast dissociation processes.

ACKNOWLEDGMENTS

We are grateful to Professor L. Delbouille and Dr. G. Roland for performing various checks on the quality

of our Fourier transforms and for pointing out possible pitfalls. One of us (J.C.L.) is indebted to Professor E. Heller for an interesting discussion. We thank the Belgian Government (Action de Recherche Concertée) and the Fonds de la Recherche Fondamentale Collective for financial support.

APPENDIX

We indicate below a simplified derivation of Eq. (I.1).

Apply the completeness relation to the set of eigenstates $|E'\rangle$ of a molecular Hamiltonian H and make use of the analytical expression of a Dirac δ function[32]

$$\int dE' \,|E'\rangle\langle E'| = 1 \quad ,$$

$$\int dE' \,\delta(E-H)\,|E'\rangle\langle E'| = \delta(E-H) \quad ,$$

$$\int dE' \,\delta(E-E')\,|E'\rangle\langle E'| = (2\pi)^{-1}\int_{-\infty}^{+\infty} \exp[i(E-H)t/\hbar]\,dt \quad ,$$

$$|E\rangle\langle E| = (2\pi)^{-1}\int_{-\infty}^{+\infty} e^{iEt/\hbar}\, e^{-iHt/\hbar}\,dt \quad . \tag{A1}$$

Consider an electronic transition of dipolar origin. Its intensity is determined by the transition moment. It is convenient, but not necessary,[4] to assume that the latter can be split into an electronic and a vibrational part, according to the Condon approximation.[33]

$$I(E) \propto E\,|R_{if}(E)|^2 = E\,\overline{M_{if}^{el}}^2\,|\langle 0|E\rangle|^2 \quad ,$$

where $\overline{M_{if}^{el}}$ is the electronic part of the transition moment (i.e., a constant quantity); $|0\rangle$ and $|E\rangle$ are now pure vibrational wave functions of the lower and upper electronic states, respectively. Then, making use of Eq. (A1)

$$I(E)/E \propto \langle 0|E\rangle\langle E|0\rangle = (2\pi)^{-1}\int_{-\infty}^{+\infty} e^{iEt/\hbar}\langle 0|e^{-iHt/\hbar}|0\rangle\,dt \quad ,$$

where H is the nuclear Hamiltonian of the excited state. When transferred on the potential energy surface of the upper state, ket $|0\rangle$ represents the initial position of the wave packet ϕ at time $t=0$, whereas $e^{-iHt/\hbar}|0\rangle$ represents the wave packet at time t as it propagates on the upper potential energy surface. Then,

$$I(E)/E \propto \int_{-\infty}^{+\infty} e^{iEt/\hbar}\langle\phi|\,\phi(t)\rangle\,dt \quad . \tag{A2}$$

Equation (I.1) follows upon inversion of the Fourier transform and normalization.

[1] R. D. Levine, *Quantum Mechanics of Molecular Rate Processes* (Clarendon, Oxford, 1969), p. 293.
[2] R. G. Gordon, Adv. Magn. Reson. 3, 1 (1968).
[3] R. T. Bailey, in *Molecular Spectroscopy*, edited by R. F. Barrows, D. A. Long, and D. J. Millen (The Chemical Society, London, 1974), Vol. 2, p. 173.
[4] E. J. Heller, J. Chem. Phys. 68, 2066, 3891 (1978). See also, K. C. Kulander and E. J. Heller, *ibid.* 69, 2439 (1978); E. J. Heller, E. B. Stechel, and M. J. Davis, *ibid.* 73, 4720 (1980); M. J. Davis, E. B. Stechel, and E. J. Heller, Chem. Phys. Lett. 76, 21 (1980); E. J. Heller, in *Potential Energy Surfaces and Dynamics Calculations*, edited by D. Truhlar (Plenum, New York, 1981); R. C. Brown and E. J. Heller, J. Chem. Phys. 75, 186 (1981).
[5] D. Bohm, *Quantum Theory* (Prentice Hall, Englewood Cliffs, 1951), p. 158.
[6] A. Messiah, *Mécanique Quantique* (Dunod, Paris, 1969), Vol. 1, pp. 126, 341.
[7] L. S. Cederbaum, W. Domcke, and H. Köppel are currently studying the relaxation of the $\tilde{A}^2B_{3g}$ state of $C_2H_4^+$ along similar lines (private communication).
[8] C. Ottinger, Z. Naturforsch. Teil A 22, 20 (1967); H. D. Beckey, H. Hey, K. Levsen, and G. Tenschert, Int. J. Mass Spectrom. Ion Phys. 2, 101 (1969); H. Tatarczyk and V. von Zahn, Z. Naturforsch. Teil. A 27, 1646 (1972); P. J. Derrick, in *Mass Spectrometry, MTP International Review of Science, Physical Chemistry Series One*, edited by A. Maccoll (Butterworths, London, 1975), Vol. 5, p. 1; P. J. Derrick and A. L. Burlinghame, Acc. Chem. Res. 7, 328 (1974); N. M. M. Niblering, Ann. Chim. (Rome) 71, 3 (1981).
[9] J. P. Hansoul, C. Calloy, and J. C. Lorquet, J. Chem. Phys. 68, 4105 (1978).
[10] M. Vaz Pires, C. Galloy, and J. C. Lorquet, J. Chem. Phys. 69, 3242 (1978); J. C. Lorquet, Adv. Mass. Spectrom. A 8, 3 (1980); J. C. Lorquet, D. Dehareng, C. Sannen, and G. Raseev, J. Chim. Phys. Phys.-Chim. Biol. 77, 719 (1980); J. C. Lorquet, J. Am. Chem. Soc. 102, 7976 (1980); C. Sannen, G. Raseev, C. Galloy, G. Fauville, and J. C. Lorquet, J. Chem. Phys. 74, 2402 (1981).
[11] G. Arfken, *Mathematical Methods for Physicists* (Academic, New York, 1970), p. 681.
[12] W. A. Steele, J. Chem. Phys. 38, 2411 (1963).
[13] A. K. Agrawal and S. Yip, Phys. Rev. 171, 263 (1968).
[14] F. Bliot, C. Abbar, and E. Constant, Mol. Phys. 24, 241 (1972).
[15] A. G. Saint-Pierre and W. A. Steele, Phys. Rev. 184, 172 (1969).
[16] W. G. Rothschild, J. Chem. Phys. 52, 6453 (1970); 53, 3265 (1970).
[17] I. Laulicht and S. Meirman, J. Chem. Phys. 59, 2521 (1973).
[18] J. Schroeder, V. H. Schierman, and J. Jonas, J. Chem. Phys. 69, 5479 (1978).
[19] R. B. Walker and R. K. Preston, J. Chem. Phys. 67, 2017 (1977).
[20] J. W. Rabalais, *Principles of Ultraviolet Photoelectron Spectroscopy* (Wiley, New York, 1977). p. 32.
[21] P. M. Dehmer and J. L. Dehmer, J. Chem. Phys. 70, 4574 (1979).
[22] Reference 20, p. 34.
[23] D. Roy, D. Dubé, M.-J. Hubin-Franskin, and J. Delwiche (unpublished results).
[24] A. Savitzky and M. E. Golay, Anal. Chem. 36, 1627 (1964); J. Steinier, Y. Termonia, and J. Deltour, *ibid.* 44, 1909 (1972).
[25] P. Barthélemy, Mémoire de Licence, Université de Liège, 1981.
[26] L. I. Schiff, *Quantum Mechanics* (McGraw-Hill, New York, 1968), p. 74.
[27] R. Bracewell, *The Fourier Transform and Its Applications* (McGraw-Hill, New York, 1965), p. 197.
[28] B. Rosen, *International Tables of Selected Constants* (Pergamon, Oxford, 1970).
[29] C. Fridh and L. Åsbrink, J. Electron Spectrosc. Relat. Phenom. 7, 119 (1975).
[30] F. Duschinsky, Acta Physicochim. URSS 7, 551 (1937).
[31] D. Dehareng, X. Chapuisat, J. C. Lorquet, C. Galloy, and G. Raseev, J. Chem. Phys. (submitted).
[32] Reference 7, p. 399.
[33] G. Herzberg, *Molecular Spectra and Molecular Structure. I. Spectra of Diatomic Molecules* (Van Nostrand, Princeton, 1966), p. 200.